EARTHQUAKE ENGINEERING AND STRUCTURAL DYNAMICS, VOL. 25, 689–709 (1996)

THE FORMATION OF VISCOUS DAMPING MATRICES FOR THE DYNAMIC ANALYSIS OF MDOF SYSTEMS

ANNA FERIANI AND FEDERICO PEROTTI

Department of Civil Engineering, University of Brescia, Via Branze 38, 25123 Brescia, Italy

SUMMARY

The paper deals with the representation of dissipative effects by means of equivalent viscous forces. A brief review of the classical analytical treatment of the subject is first presented devoting particular attention to the topics of hysteretic and modal damping. The problem of forming viscous matrices in the case of systems which are non-homogeneous from the point of view of dissipation is then addressed; soil–structure systems are first considered and some accepted techniques for forming the structure contribution to the viscous matrix are reviewed. A different technique is then proposed which avoids some of the drawbacks of the previously quoted methods. In the final section of the paper it is shown how this technique is easily applicable also in the case of systems having internal concentrated dampers of viscous type, this being a situation which is difficult to tackle with usual criteria.

KEY WORDS: structural dynamics, damping modelling

1. INTRODUCTION

The problem of consistent representation of dissipative effects has not received, among researchers who work in the field of dynamic structural analysis, the same degree of attention which has been devoted to other aspects of material and structural elements modelling. This is largely justified by several considerations which we will try to summarize in the following:

(a) In dynamic linear time-domain analysis dissipation modelling is restricted to the viscous mechanism, which is a very crude and not easily workable assumption for most damping effects.
(b) In dynamic linear frequency-domain analysis, the combination of viscous and hysteretic damping allows, under some well-accepted hypotheses and approximations, to accomodate in an easier and more realistic way a wider range of dissipation effects.
(c) In dynamic non-linear analysis the most important dissipation source, i.e. hysteretic material behaviour, can be correctly modelled by appropriate inelastic constitutive relations.

The quoted considerations support the belief that, for linear analysis, frequency domain direct algorithms can be used to better account for dissipative effects while for non-linear analysis refined constitutive laws allow for consistent modelling of the largest part of energy losses; in other words the refinement of the classical approach of reducing all dissipation effects to equivalent viscous forces does not seem to deserve a great deal of interest, at least for practical purposes.

On the other hand, even if focusing the attention on linear problems, promising time-domain techniques have been developed to deal with arbitrarily modelled viscous damping; for example, the performance of complex modal analysis for decoupling problems with non-proportional damping has been extensively studied, in the last decades, both from the analytical and the numerical point of view (see References 1–5). The same degree of attention, however, has not been dedicated to the problem of the formation of the damping matrix.

More generally, it must be noted that, in terms of numerical efficiency in treating 'large' problems, the challenge between direct frequency-domain techniques and time-domain analysis via the complex modes of

CCC 0098–8847/96/070689–21

Received 18 July 1995
Revised 5 February 1996

the damped system is still an open one; in many cases the actual advantage of frequency analysis lies in its better flexibility to deal with dissipative effects. Modal analysis, on the other hand, gives a better insight into the system behaviour and allows for the direct use of well-established analysis tools, such as response spectra in seismic analysis.

As far as inelastic analysis is concerned, it can be argued, in response to the above comments, that complete non-linear modelling of complex soil–structure systems is still a formidable task, so that non-linear behaviour is often considered for structural elements only, while soil behaviour is linearized and non-structural elements stiffness and resistance is simply neglected. This means that in most non-linear dynamic analyses viscous forces still play a significant role, since they must account for dissipations in all linearly modelled materials, including elastic branches of piecewise-linear hysteretic rules characterizing the behaviour of inelastic elements.

Summing up, the problem of consistent formation of damping matrices seemed to deserve, in the writers' opinion, some research effort, whose results are described in the present paper.

In the first part of the paper standard techniques for linear dissipation modelling are reviewed for clarity of the subsequent presentation. The physical aspects of energy dissipation in linearly modelled dynamical systems are then briefly summarized.

The remaining part of the paper is devoted to the discussion of different techniques for assembling viscous damping matrices for typical systems encompassing different sources of dissipation, such as soil–structure systems or systems with concentrated viscous dampers.

2. MODELLING OF DISSIPATIVE EFFECTS IN LINEAR STRUCTURAL DYNAMICS

2.1. *Viscous and hysteretic damping*

The equations of motion of an n-DOF linear system can be written in the matrix form

$$\mathbf{m}\ddot{\mathbf{q}} + \mathbf{c}\dot{\mathbf{q}} + \mathbf{k}\mathbf{q} = \mathbf{Q} \tag{1}$$

$\mathbf{q}$ being the vector of Lagrangian coordinates, $\mathbf{Q}$ the vector of generalized components of dynamic forces, $\mathbf{m}$ and $\mathbf{k}$ the inertia and stiffness matrices, respectively, while $\mathbf{c}$ is the viscous damping matrix. In the case of complex harmonic excitation, the system (1) takes the form

$$\mathbf{m}\ddot{\mathbf{q}} + \mathbf{c}\dot{\mathbf{q}} + \mathbf{k}\mathbf{q} = \mathbf{F}e^{i\omega t} \tag{2}$$

Equations (2) admit the steady-state solution

$$\mathbf{q}(t) = \mathbf{H}_V(\omega)\mathbf{F}e^{i\omega t} \tag{3}$$

where $\mathbf{H}_V(\omega)$ is the following matrix of complex frequency-response functions:

$$\mathbf{H}_V(\omega) = [-\omega^2\mathbf{m} + \mathbf{k} + i\omega\mathbf{c}]^{-1} \tag{4}$$

Within the context of steady-state harmonic analysis, inverse proportionality between the damping matrix and the circular frequency can be stated as

$$\mathbf{c} = \frac{1}{|\omega|}\mathbf{c}_H \tag{5}$$

in which the $\mathbf{c}_H$ matrix is named 'hysteretic' damping matrix. Upon substitution of expression (5), the frequency-response matrix takes the form

$$\mathbf{H}_H(\omega) = [-\omega^2\mathbf{m} + \mathbf{k} + i\,\mathrm{sign}\,(\omega)\mathbf{c}_H]^{-1} \tag{6}$$

When compared to the viscous one the linear hysteretic (LH) damping model (5) is thought to be in better accordance with experimental results concerning structural elements under harmonic loading, since it leads to an amount of dissipated energy per cycle W_D which is independent of frequency ω, while the viscous model results in linear variation of the function $W_D(\omega)$.

For a system which is homogeneous in terms of dissipation, the hysteretic matrix can be stated as proportional to the stiffness matrix according to the damping factor μ, i.e.,

$$\mathbf{c}_{\mathrm{H}} = \mu \mathbf{k}$$

For non-homogeneous systems, proportionality can be stated at the subsystem or element level; by denoting with $\mu^{(k)}$ the hysteretic damping factor of the kth subsystem (or element) and with $\mathbf{c}_{\mathrm{H}}^{(k)}$ and $\mathbf{k}^{(k)}$ its contributions to the hysteretic damping matrix and to the stiffness matrix, respectively, we can derive, for the global system composed of m subsystems, the following matrices:

$$\mathbf{k} = \sum_{k=1}^{m} \mathbf{k}^{(k)}, \qquad \mathbf{c}_{\mathrm{H}} = \sum_{k=1}^{m} \mathbf{c}_{\mathrm{H}}^{(k)} = \sum_{k=1}^{m} \mu^{(k)} \mathbf{k}^{(k)} \tag{7}$$

The possibility of using the LH model for the case of transient excitation has been thoroughly debated during the last decades (see Reference 6 for a recent state-of-the-art discussion of the topic). More precisely it has been pointed out that the model violates the requirement of causality of mechanical systems (see References 7–9 for interesting discussions of the topic).

For a brief illustration of the problem, which has been treated more extensively in Reference 10, let us consider a SDOF system; in this case the unit-impulse response function can easily be evaluated, by the FFT technique, as the inverse Fourier Transform of the frequency-response function. The latter function, for the hysteretic case, takes the form:

$$\mathbf{H}_{\mathrm{H}}(\omega) = \frac{1}{k}\left[1 - \frac{\omega^2}{\omega_1^2} + \mathrm{i}\,\mathrm{sign}\,(\omega)\mu\right]^{-1} \tag{8}$$

where ω_1 is the natural circular frequency and k the stiffness of the system.

Some tests have been performed (see again Reference 10) for a linear oscillator having natural frequency equal to 2·5 Hz, unit stiffness and different values of the hysteretic damping factor. The unit-impulse response function $h_{\mathrm{H}}(t)$ has been evaluated for the time interval $-5\,\mathrm{s} < t < 5\,\mathrm{s}$ (frequency step equal to 0·1 Hz) at time steps of 0·01 s (folding frequency equal to 50 Hz); as an example, the function obtained for the case $\mu = 0{\cdot}2$ is shown in Figure 1 along with the analytical unit-impulse response $h_{\mathrm{V}}(t)$ of a viscous oscillator having the same natural frequency and a damping factor equal to 0·1, this choice leading to the same magnification at resonance. As it can be noted the two functions are in close agreement for $t > 0$; for negative times, however, significant response is shown by the hysteretic oscillator, even though limited to a short time interval.

By an analytical point of view several criteria can be applied to test the lack of causality of the hysteretic impulse function (see e.g. References 11 and 12). It can also be noted that by separating the real and imaginary part of $\mathbf{H}_{\mathrm{H}}(\omega)$ as

$$\mathbf{H}_{\mathrm{H}}(\omega) = X(\omega) + \mathrm{i}Y(\omega) \tag{9}$$

the inverse transform $h_{\mathrm{X}}(t)$ of the continuous function $X(\omega)$ can be obtained via integration in the complex plane, obtaining the following result:

$$h_{\mathrm{X}}(t) = \frac{\exp(-|t|\omega_{\mathrm{H}}\sin\theta)[-\sin\theta\cos(|t|\omega_{\mathrm{H}}\cos\theta) + \cos\theta\sin(|t|\omega_{\mathrm{H}}\cos\theta)]}{2m\omega_{\mathrm{H}}} \tag{10}$$

where

$$\omega_{\mathrm{H}} = \omega_1(1+\mu^2)^{0{\cdot}25}, \qquad \cos(2\theta) = \frac{1}{\sqrt{1+\mu^2}}, \qquad \sin(2\theta) = \frac{\mu}{\sqrt{1+\mu^2}}$$

As to the imaginary part $Y(\omega)$ it can be demonstrated that its inverse transform $h_Y(t)$ is everywhere continuous[12] over $(-\infty, \infty)$. Since $Y(\omega)$ and, therefore, $h_Y(t)$ are odd, we can state $h_Y(0) = 0$, so that $h_{\mathrm{H}}(0) = h_{\mathrm{X}}(0)$; in Figure 2 the non-dimensional value of $h_{\mathrm{H}}(0)$, as computed from equation (10), is plotted as a function of the hysteretic damping factor μ.

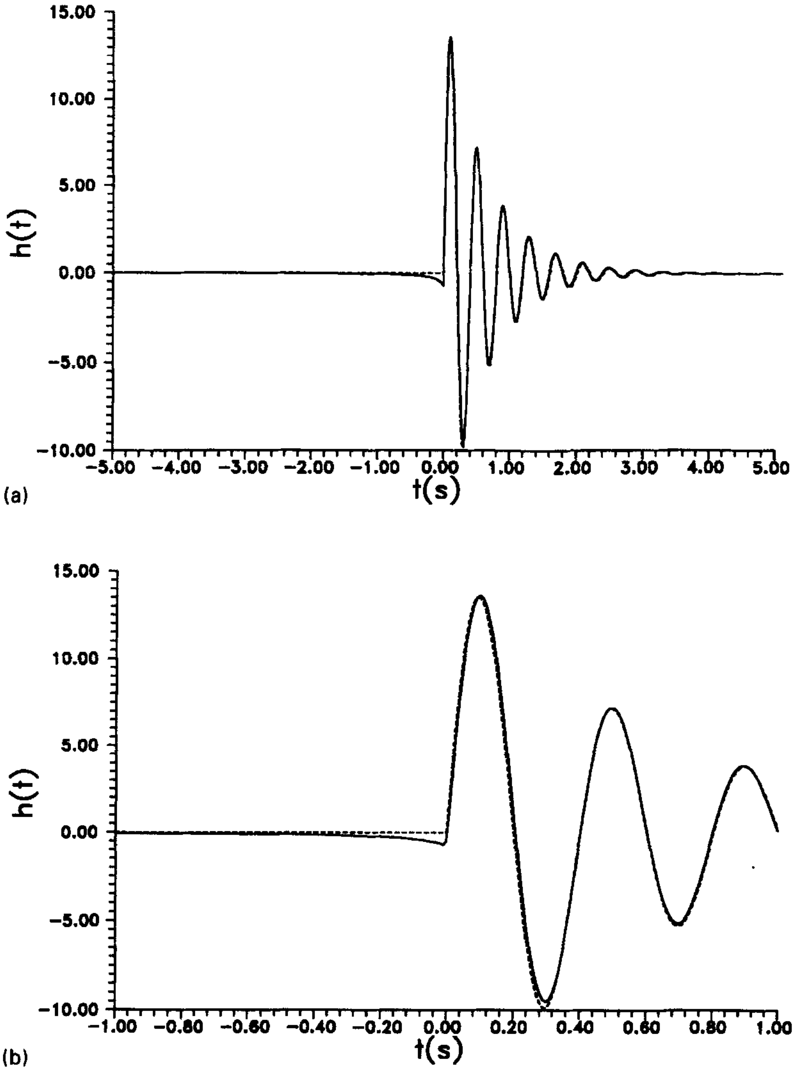

Figure 1. (a) Unit-impulse response functions for hysteretic and viscous SDOF systems; $\mu = 0{\cdot}2$ (——) hysteretic, (----) viscous. (b) Enlarged portion of Figure 1(a)

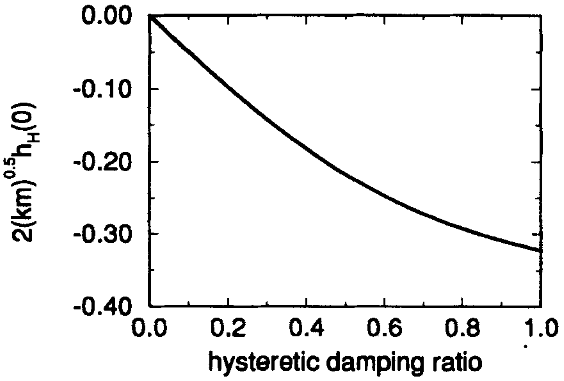

Figure 2. Analytically computed unit-impulse response function for hysteretic SDOF system: value at $t = 0$ vs. hysteretic damping ratio

2.2. Modal and weighted damping

Going back to our original viscous model, assume that the classical modes of the system, that is the eigenpairs ($\omega_j, \boldsymbol{\phi}_j$, $j = 1, \ldots, n$) are known. Assuming damping proportionality the equations of motion can be re-written in the decoupled form

$$\ddot{y}_j + 2\zeta_j \omega_j \dot{y}_j + \omega_j^2 y_j = \frac{\boldsymbol{\phi}_j^{\mathrm{T}} \mathbf{Q}}{\boldsymbol{\phi}_j^{\mathrm{T}} \mathbf{m} \boldsymbol{\phi}_j}, \quad j = 1, \ldots, n \tag{11}$$

where modal damping factors ζ_j are defined as

$$\zeta_j = \frac{1}{2\omega_j} \frac{\boldsymbol{\phi}_j^{\mathrm{T}} \mathbf{c} \boldsymbol{\phi}_j}{\boldsymbol{\phi}_j^{\mathrm{T}} \mathbf{m} \boldsymbol{\phi}_j} \tag{12}$$

For homogeneous structural systems the modal damping factors can be set equal for all normal modes; for non-homogeneous systems approximate procedures are available. The most classical approach, proposed by Roesset *et al.*,[13] considers a linear system encompassing n_{H} hysteretic structural subsystems, each of them characterized by damping factor $\mu^{(m)}$, and n_{V} spring-damper (viscous) subsystems, each of them characterized by damping coefficient $c^{(l)}$ and stiffness $k^{(l)}$. The method allows for the statement of energy consistent modal damping factors, in the following form:

$$\zeta_j = \frac{1}{2} \frac{\sum_{l=1}^{n_{\mathrm{V}}} \omega_j \frac{c^{(l)}}{k^{(l)}} E_{\mathrm{MAX},j}^{(l)} + \sum_{m=1}^{n_{\mathrm{H}}} \mu^{(m)} E_{\mathrm{MAX},j}^{(m)}}{\sum_{l=1}^{n_{\mathrm{V}}} E_{\mathrm{MAX},j}^{(l)} + \sum_{m=1}^{n_{\mathrm{H}}} E_{\mathrm{MAX},j}^{(m)}} \tag{13}$$

where

$$E_{\mathrm{MAX},j}^{(k)} = \tfrac{1}{2} \boldsymbol{\phi}_j^{\mathrm{T}} \mathbf{k}^{(k)} \boldsymbol{\phi}_j$$

For a purely hysteretic and homogeneous system ($\mu^{(m)} = \mu$ for $m = 1, \ldots, n_{\mathrm{H}}$) equation (13) gives the standard result $\zeta_j = \mu/2$; for a totally viscous system ($n_{\mathrm{H}} = 0$) the same result as obtained by equation (12) is obtained.

Finally, a viscous damping matrix can be computed, under the proportionality assumption and starting from the modal damping factors, according to the well-known formula (see Reference 14)

$$\mathbf{c}_{\mathrm{V}} = \mathbf{m} \left[\sum_{j=1}^{p} \boldsymbol{\phi}_j \boldsymbol{\phi}_j^{\mathrm{T}} \frac{2\zeta_j \omega_j}{M_j} \right] \mathbf{m} \tag{14}$$

where $M_j = \boldsymbol{\phi}_j^{\mathrm{T}} \mathbf{m} \boldsymbol{\phi}_j$ and where $p \leqslant n$ is the number of normal modes included in the analysis. Note that the damping matrix (14) is positive definite only for $p = n$, otherwise oscillations due to normal modes higher than the pth are undamped.

2.3. The physical viewpoint

Equivalent viscous forces are introduced in structural *linear* dynamics computations to take into account a number of dissipative effects, namely

(a) structural elements hysteresis,
(b) non-structural elements hysteresis,
(c) structural joints behaviour,
(d) foundation medium hysteresis,
(e) foundation medium wave radiation,
(f) dissipation due to concentrated damping devices.

Examination of the above list suggests the following considerations.

(i) effects from (a) to (d), which are due to actual non-linear behaviour of materials that are modelled as elastic (or rigid as often done for joints), are best suitable for the hysteretic model;

(ii) in many situations the wave radiation effect (e) can be modelled, with acceptable approximation, in terms of concentrated viscous dampers having constant properties (i.e. independent of frequency): these dampers are located at the contact nodes between the foundation and the surrounding medium or at the boundary nodes of the ground finite-element mesh;
(iii) concentrated damping devices can be of viscous type.

The above considerations point out how distributed dissipation effects, related to structural materials behaviour, tend to be of hysteretic type, while viscous effects are related to concentrated devices, even though fictitious as in the case of the radiation damping.

In the case of *non-linear* dynamic analysis, viscous forces are introduced essentially for the same reasons; the main difference is that the hysteretic model cannot be employed since time-domain analysis must be performed. Secondly, viscous dissipation becomes less important in comparison with the dissipation associated with inelastic cycling of non-linear elements.

Regarding the data which are usually available for modelling the above listed effects, they can be summarized as follows:

(1) damping factors for representing hysteretic dissipation in structures or foundation media;
(2) damping coefficients, assumed constant, for representing wave radiation damping in a foundation medium;
(3) damping coefficients for concentrated damping devices.

The problem of forming viscous damping matrices starting from these data and capturing, as well as possible, the physical aspects of dissipation are the object of the next sections.

The results obtained, in terms of frequency-response functions, from different techniques for viscous matrix formation will be compared with the one resulting from the use of hysteretic structural damping combined with the effect of concentrated dashpots to represent viscous effects (Combined Viscous and Linear Hysteretic model (CVLH) in the following). The choice of the CVLH model as a benchmark for equivalent viscous modelling appears to be justified by its adequacy to physical dissipation properties of structural elements and by its consistency in the treatment of non-homogeneous systems.

As it concerns the above-discussed theoretical problems regarding the use of hysteretic damping for transient loading, it can be noted that the various models of energy dissipation are here compared in terms of frequency-response functions only, i.e. still in the context of steady-state harmonic loading. More generally, it can be observed that the LH approach is usually applied to model hysteretic dissipation in structural elements or foundation media; these phenomena are generally characterized by small damping values, such that the non-causal behaviour of the LH model appears to be of little importance.

3. THE FORMATION OF VISCOUS DAMPING MATRICES FOR STRUCTURAL SYSTEMS INTERACTING WITH THE FOUNDATION GROUND

3.1. Structures on rigid mat foundation

A case which is frequently encountered in civil engineering dynamics is the one of a structure which is homogeneous by the point of view of dissipation but interacts with a foundation medium having totally different damping properties; the situation of rigid mat foundations is addressed here first. The data about system dissipation are, in this case, the structural hysteretic damping factor $\mu^{(s)}$, the ground hysteretic damping factor $\mu^{(g)}$ and the coefficients of the viscous dashpots modelling soil radiation damping.

Accepted techniques, in such cases, for forming a viscous damping matrix are based upon the hypothesis, which is consistent with the hysteretic structural behaviour, that energy dissipation in the structure is dependent on motions encompassing deformations of its elements while rigid-body motions allowed by deformability of the ground cause dissipation only in the latter medium.

Considering this, structural damping can be associated, as a first alternative, to the velocities $\dot{\mathbf{q}}_r^{(sf)}$ relative to the foundation mat. Under this hypothesis and assuming modal structural damping factors $\zeta^{(s)} = \frac{1}{2}\mu^{(s)}$, the damping matrix can be obtained performing the following steps.

(1) The damping matrix $\bar{\mathbf{c}}_V^{(sf)}$ for the fixed-base structure is computed, from the damping factor μ_s, according to expression (14) as

$$\bar{\mathbf{c}}_V^{(sf)} = \mathbf{m}^{(sf)} \left[\sum_{j=1}^{p_s} \boldsymbol{\phi}_j^{(sf)} \boldsymbol{\phi}_j^{(sf)T} \frac{2\zeta^{(s)}\omega_j^{(sf)}}{M_j^{(sf)}} \right] \mathbf{m}^{(sf)} \tag{15}$$

where the superscript (sf) denotes fixed-base structural properties and eigenpairs.

(2) The transformation

$$\dot{\mathbf{q}}_r^{(sf)} = \boldsymbol{\alpha}\dot{\mathbf{q}} \tag{16}$$

is computed between velocities relative to the moving reference $\dot{\mathbf{q}}$ and velocities relative to the foundation mat $\dot{\mathbf{q}}_r^{(sf)}$.

(3) To define the structure damping matrix $\mathbf{c}_V^{(s)}$ in the $\mathbf{q}$ coordinate system, the Rayleigh dissipation function is then expressed, according to the above hypothesis, as

$$D^{(s)} = \tfrac{1}{2}\dot{\mathbf{q}}_r^{(sf)T}\bar{\mathbf{c}}_V^{(sf)}\dot{\mathbf{q}}_r^{(sf)} = \tfrac{1}{2}\dot{\mathbf{q}}^T\boldsymbol{\alpha}^T\bar{\mathbf{c}}_V^{(sf)}\boldsymbol{\alpha}\dot{\mathbf{q}} \tag{17}$$

which implicitly defines $\mathbf{c}_V^{(s)}$ as

$$\mathbf{c}_V^{(s)} = \boldsymbol{\alpha}^T\bar{\mathbf{c}}_V^{(sf)}\boldsymbol{\alpha} \tag{18}$$

(4) The ground damping matrix $\mathbf{c}_V^{(g)}$ is formed according to the damping coefficients of the dashpots modelling the wave radiation effect and to the equivalent viscous damping coefficients accounting for ground hysteresis; the latter coefficients are usually determined assuming as reference frequencies the ones of rigid-body structural motions (sway, rocking about foundation centroid, etc.) due to ground deformability.

(5) The structural damping matrix $\mathbf{c}_V^{(s)}$ is finally added to the ground damping matrix $\mathbf{c}_V^{(g)}$ to form the total viscous damping matrix

$$\mathbf{c}_V = \mathbf{c}_V^{(s)} + \mathbf{c}_V^{(g)} \tag{19}$$

An alternative to this procedure, which will be denoted as FSMD (Fixed Structure Modal Damping) in the following, can be derived assuming that structural damping is related to the absolute, but deformative, motions of the unrestrained structure. Under this hypothesis a new procedure, named USMD (Unrestrained Structure Modal Damping), is derived by re-writing expressions (15)–(18) as follows

$$\bar{\mathbf{c}}_V^{(su)} = \mathbf{m}^{(su)} \left[\sum_{j=1}^{p_s} \boldsymbol{\phi}_j^{(su)} \boldsymbol{\phi}_j^{(su)T} \frac{2\zeta^{(s)}\omega_j^{(su)}}{M_j^{(su)}} \right] \mathbf{m}^{(su)} \tag{20}$$

$$\dot{\mathbf{q}}^{(su)} = \boldsymbol{\beta}\dot{\mathbf{q}} \tag{21}$$

$$D^{(s)} = \tfrac{1}{2}\dot{\mathbf{q}}^{(su)T}\bar{\mathbf{c}}_V^{(su)}\dot{\mathbf{q}}^{(su)} = \tfrac{1}{2}\dot{\mathbf{q}}^T\boldsymbol{\beta}^T\bar{\mathbf{c}}_V^{(su)}\boldsymbol{\beta}\dot{\mathbf{q}} \tag{22}$$

$$\mathbf{c}_V^{(s)} = \boldsymbol{\beta}^T\bar{\mathbf{c}}_V^{(su)}\boldsymbol{\beta} \tag{23}$$

In the preceding expressions the superscript (su) denotes the properties of the unrestrained structure; note that in the summation (20) rigid-body modes are left out. Since no absolute–relative coordinate transformation is now necessary, the matrix $\boldsymbol{\beta}$ simply enforces compatibility conditions at the structure–foundation interface.

To test the above-described procedures the response of the cantilever structure illustrated in Figure 3, whose mechanical properties are summarized in Table I, has been computed for the case of horizontal base motion. For such a system (named system A in the following) given that the Lagrangian co-ordinates $\mathbf{q}$ are

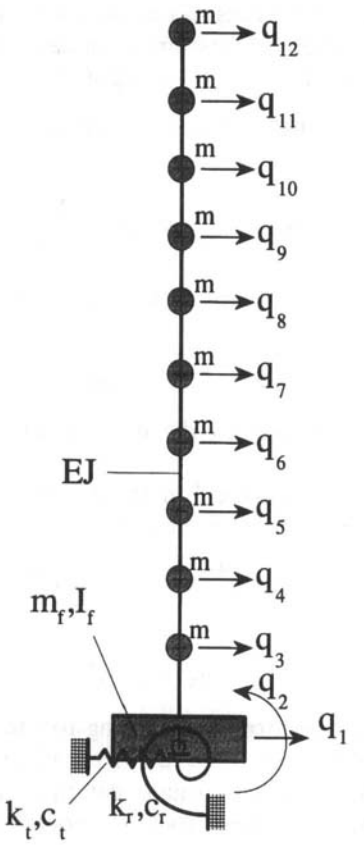

Figure 3. System A. Dynamic model

Table I. System A: mechanical properties

EJ	m	m_f	I_f	H
10^6 kN m^2	$7{\cdot}6 \times 10^3$ kg	288×10^3 kg	1520×10^3 kg m^2	1 m
k_t	k_r	c_t	c_r	$\mu^{(s)}$
48 000 kN/m	$7{\cdot}02 \times 10^5$ kN m	3056×10^3 kg/s	$16\,760 \times 10^3$ kg m^2/s	0·10

relative to the base motion and considering unit harmonic base acceleration, the generalized force vector, containing the harmonic forces amplitudes (equations (2)), is of the type

$$\mathbf{F} = -\left[\mathbf{m}^{(s)} - \frac{i}{\omega}\mathbf{c}^{(s)}\right]\mathbf{r} \tag{24}$$

where $\mathbf{r}$ is a vector containing unit components along co-ordinates which are directed as the base motion and zero components elsewhere.

Note that, due to the form of the $\mathbf{r}$ vector, the forcing term due to viscous damping is zero when the structure, as occurs in the above-described methods, dissipates no energy in rigid-body modes. In general, given expression (24), the frequency-response functions for Lagrangian co-ordinates are

$$\bar{\mathbf{q}}(\omega) = \mathbf{H}(\omega)\mathbf{F} = -\mathbf{H}(\omega)\left[\mathbf{m}^{(s)} - \frac{i}{\omega}\mathbf{c}_V^{(s)}\right]\mathbf{r} \tag{25}$$

In the case of a response parameter $s(t)$ (e.g. internal action or stress components) which is linearly related to the components of $\mathbf{q}$, i.e.,

$$s(t) = \mathbf{b}^{\mathrm{T}}\mathbf{q} \tag{26}$$

where $\mathbf{b}$ is a suitable stiffness vector, the corresponding frequency-response function becomes, from equations (25) and (26),

$$\bar{s}(\omega) = -\,\mathbf{b}^{\mathrm{T}}\mathbf{H}(\omega)\left[\mathbf{m}^{(s)} - \frac{\mathrm{i}}{\omega}\mathbf{c}_{\mathrm{V}}^{(s)}\right]\mathbf{r} \tag{27}$$

As an example, frequency-response amplitude curves have been obtained according to expression (27) and considering different dissipation models, for the top beam element shear V_{10} and for base shear V_{f} (elastic force in the translational spring).

In Figures 4 and 5 the curves obtained assuming a viscous damping matrix computed via equations (15–18) and (20–23) are compared with the ones resulting from the CVLH model (hysteretic damping for soil

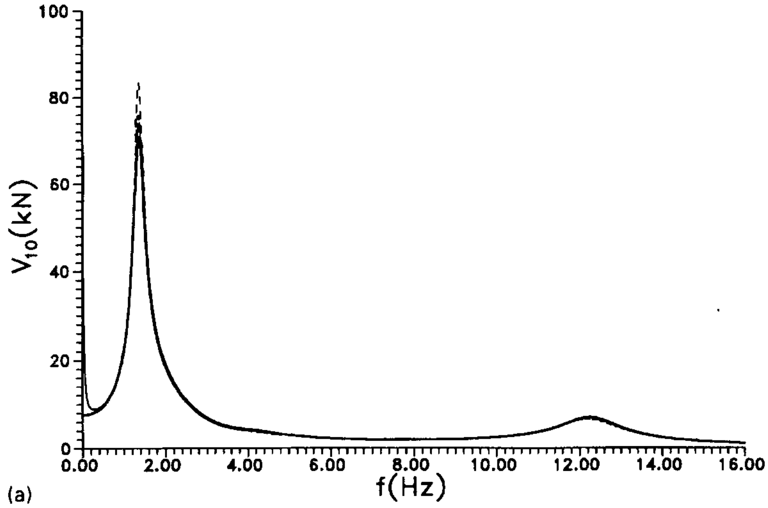

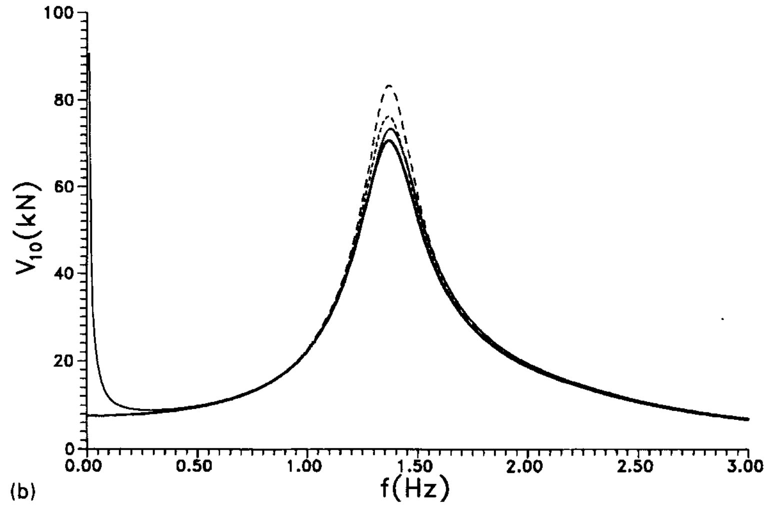

Figure 4. (a) System A. Frequency-response function amplitude for shear V_{10}: (▬) CVLH, (——) CSMD, (- - - -) FSMD, (– – – –) USMD. (b) Enlarged portion of Figure 4(a)

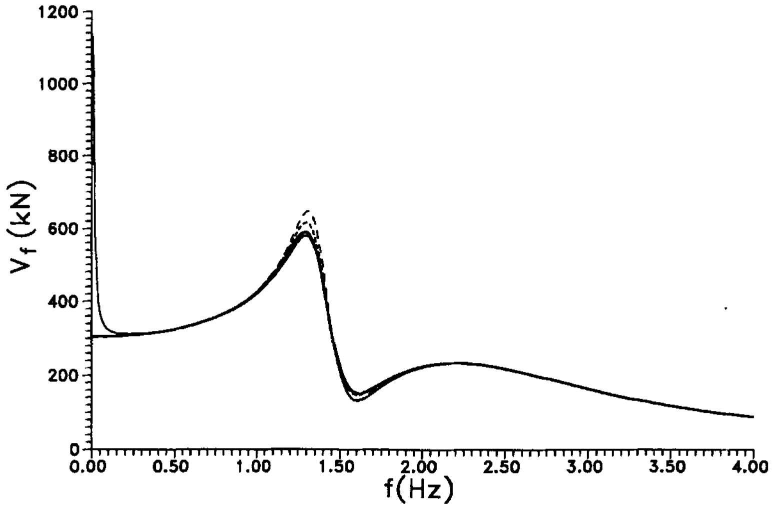

Figure 5. System A. Frequency-response function amplitude for elastic force V_f: (▬▬) CVLH, (——) CSMD, (- - - -) FSMD, (— — —) USMD

and structure internal dissipation plus viscous damping for base radiation), this resulting in the frequency-response matrix:

$$\mathbf{H}(\omega) = [-\omega^2\mathbf{m} + \mathbf{k} + \mathrm{i}\,\mathrm{sign}(\omega)[\mu^{(s)}\mathbf{k}^{(s)} + \mu^{(g)}\mathbf{k}^{(g)}] + \mathrm{i}\omega\mathbf{c}_V^{(g)}]^{-1} \tag{28}$$

where $\mathbf{k}^{(s)}$ and $\mathbf{k}^{(g)}$ denote the structure and ground contributions to the stiffness matrix. It is worth noting that in the CVLH assumption, where the structural contributions to damping forces are proportional to the elastic forces, the damping term in equation (24) annihilates. The ground hysteretic damping factor $\mu^{(g)}$ has been taken as zero in the example shown here.

As it can be noted in Figures 4 and 5 both techniques for forming equivalent viscous damping matrix fail in predicting the first mode peak amplitude; this is mainly due to the fact that matrices (15) and (20) are computed according to the natural frequencies of the fixed-base (for FSMD) and unrestrained (for USMD) structure, which are significantly different from the ones of the combined soil–structure system. This is illustrated in Table II where natural frequencies are collected; note that the values pertaining to similar modal shapes are horizontally aligned.

To overcome this problem a different technique has been tested in which the structure damping factor is associated to the normal modes of the combined system; to do this, the assumption has been made that the damping matrix resulting from the hysteretic dissipation in the structure and in the ground is proportional. According to these criteria the combined system damping matrix has been formed by performing the following steps:

(1) computation of modal damping factors taking hysteretic damping for both structure and ground into account, i.e. from expression (13), according to the weighted damping formula

$$\zeta_{j,\mathrm{H}} = \frac{1}{2}\frac{\mu^{(s)}E^{(s)}_{\mathrm{MAX},j} + \mu^{(g)}E^{(g)}_{\mathrm{MAX},j}}{E^{(s)}_{\mathrm{MAX},j} + E^{(g)}_{\mathrm{MAX},j}} \tag{29}$$

(2) computation of the viscous damping matrix $\mathbf{c}_{\mathrm{V,H}}$ equivalent to hysteretic damping as

$$\mathbf{c}_{\mathrm{V,H}} = \mathbf{m}\left[\sum_{j=1}^{p} \boldsymbol{\phi}_j\boldsymbol{\phi}_j^{\mathrm{T}}\frac{2\zeta_{j,\mathrm{H}}\omega_j}{M_j}\right]\mathbf{m} \tag{30}$$

(3) computation of the total damping matrix as

$$\mathbf{c}_{\mathrm{V}} = \mathbf{c}_{\mathrm{V,H}} + \mathbf{c}_{\mathrm{V}}^{(g)} \tag{31}$$

where $\mathbf{c}_{\mathrm{V}}^{(g)}$ accounts, in this case, only for radiation damping effects.

Table II. System A: natural frequencies (Hz) for different constraint conditions

Combined system		Fixed-base structure		Unrestrained structure	
1	1·342	1	1·845	1	0·000
2	2·323			2	0·000
3	4·291			3	3·131
4	12·28	2	11·62	4	12·25
5	33·15	3	32·69	5	33·14
6	64·72	4	64·30	6	64·72
7	106·9	5	106·5	7	106·9
8	159·1	6	158·7	8	159·1
9	219·6	7	219·2	9	219·6
10	283·8	8	283·5	10	283·8
11	343·0	9	342·8	11	343·0
12	385·0	10	384·9	12	385·0

Note that the modal properties appearing in equations (29) and (30) are now the ones of the combined system. It is also important to observe that the structure contribution to the $\mathbf{c}_{V,H}$ matrix, which can be obtained from equations (29) and (30) by setting $\mu^{(g)} = 0$, is not a singular matrix, so that its product by the $\mathbf{r}$ vector gives a non-zero forcing term in equation (24); from a physical point of view this amounts to the undesirable property that structural dissipation is governed by velocities relative to the moving reference instead of velocities relative to the foundation mat. This fact is obviously of concern only in the moving reference case: if constraints are fixed and dynamic forces are actually applied on the system, as occurs in the case of wind forces or vibrating machines, no problem arises in using the damping matrix (30).

The frequency-response amplitude curve for a damping matrix computed according to equations (29)–(31), which will be termed as CSMD (Combined System Modal Damping) procedure, is again illustrated in Figures 4 and 5 for the same response parameters. It can be noted how, in the intermediate and high-frequency range, the agreement between these curves and the curves obtained assuming the CVLH model is better than the one achieved by means of the previously quoted criteria (FSMD and USMD).

In the low-frequency range, however, the effect of the structural damping term in the excitation gives rise to spurious results due to the presence of the $1/\omega$ factor in equation (24); we remind that the CSMD technique is the only, among the ones here tested, for which the damping term does not disappear from the equivalent forces vector (24). To test the importance of this term, frequency-response functions have been computed also by neglecting it (inertial excitation). The result is shown in Figures 6 and 7 (where it is termed 'CSMD-inertial') and demonstrates how the influence of damping contribution in the excitation vector is not significant except in the very low-frequency range and how in the same range the curves obtained by the inertial excitation assumption are in very good agreement with the one resulting from the CVLH model.

Note that the CSMD procedure (29)–(31) remains the same as here sketched even in the case that a FEM with viscous boundaries is adopted for the ground medium. With the other procedures, on the other hand, a method similar to the one adopted for the structural system must be used to build a viscous matrix equivalent to the hysteretic ground effect.

3.2. *Multiply-supported structures*

The formation of an equivalent viscous damping matrix involves some additional aspects in the case of multiply-supported structures under differential ground motions; this is a frequently encountered problem in the field of bridge and lifeline engineering. In the case of surface foundations, the absolute motion $\mathbf{q}(t)$ of such systems can be studied by expressing the configuration vector as the sum of the free-field motion $\mathbf{q}_f(t)$ and of

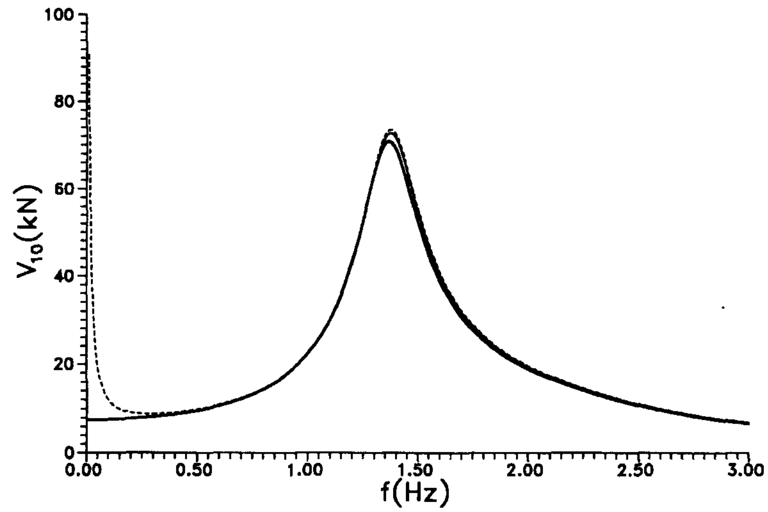

Figure 6. System A. Frequency-response function amplitude for shear V_{10}: (▬) CVLH, (——) CSMD-inertial, (- - - -) CSMD

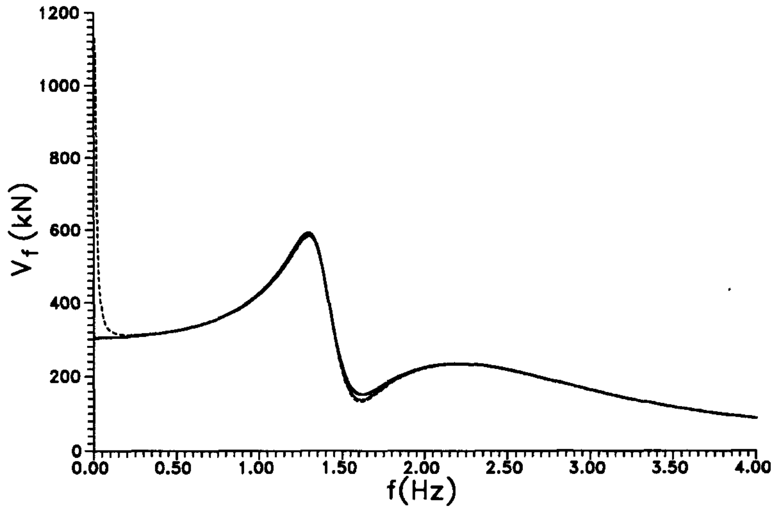

Figure 7. System A. Frequency-response function amplitude for elastic force V_f. (▬) CVLH, (——) CSMD-inertial, (- - - -) CSMD

the so-called 'added' motion $\mathbf{q}_a(t)$ and then partitioning the configuration vectors into three subvectors listing structural, 'contact' and ground co-ordinates, i.e.,

$$\mathbf{q} = \mathbf{q}_a + \mathbf{q}_f; \qquad \mathbf{q}_a = \begin{Bmatrix} \mathbf{q}^{(s)} \\ \mathbf{q}_a^{(c)} \\ \mathbf{q}_a^{(g)} \end{Bmatrix}; \qquad \mathbf{q}_f = \begin{Bmatrix} \mathbf{0} \\ \mathbf{u} \\ \mathbf{q}_f^{(g)} \end{Bmatrix} \tag{32}$$

where $\mathbf{u}$ is the vector listing the free-field motions at the soil–structure contact points.

According to the partition (32) the matrices expressing the structure contributions to the inertia, damping and stiffness matrices of the combined system can be expressed as follows:

$$\mathbf{m}^{(s)} = \begin{bmatrix} \mathbf{m}_{ss}^{(s)} & \mathbf{m}_{sc}^{(s)} & \mathbf{0} \\ \mathbf{m}_{cs}^{(s)} & \mathbf{m}_{cc}^{(s)} & \mathbf{0} \\ \mathbf{0} & \mathbf{0} & \mathbf{0} \end{bmatrix}; \quad \mathbf{c}^{(s)} = \begin{bmatrix} \mathbf{c}_{ss}^{(s)} & \mathbf{c}_{sc}^{(s)} & \mathbf{0} \\ \mathbf{c}_{cs}^{(s)} & \mathbf{c}_{cc}^{(s)} & \mathbf{0} \\ \mathbf{0} & \mathbf{0} & \mathbf{0} \end{bmatrix}; \quad \mathbf{k}^{(s)} = \begin{bmatrix} \mathbf{k}_{ss}^{(s)} & \mathbf{k}_{sc}^{(s)} & \mathbf{0} \\ \mathbf{k}_{cs}^{(s)} & \mathbf{k}_{cc}^{(s)} & \mathbf{0} \\ \mathbf{0} & \mathbf{0} & \mathbf{0} \end{bmatrix} \tag{33}$$

Given the above definitions the dynamic equilibrium equations, in terms of the added motion, can be written in the following form (see e.g. Reference 15):

$$\mathbf{m}\ddot{\mathbf{q}}_a + \mathbf{c}\dot{\mathbf{q}}_a + \mathbf{k}\mathbf{q}_a = -\begin{bmatrix} \mathbf{m}_{sc}^{(s)} \\ \mathbf{m}_{cc}^{(s)} \\ \mathbf{0} \end{bmatrix} \ddot{\mathbf{u}} - \begin{bmatrix} \mathbf{c}_{sc}^{(s)} \\ \mathbf{c}_{cc}^{(s)} \\ \mathbf{0} \end{bmatrix} \dot{\mathbf{u}} - \begin{bmatrix} \mathbf{k}_{sc}^{(s)} \\ \mathbf{k}_{cc}^{(s)} \\ \mathbf{0} \end{bmatrix} \mathbf{u} \tag{34}$$

Note that the inertia, damping and stiffness matrices ($\mathbf{m}$, $\mathbf{c}$ and $\mathbf{k}$, respectively) appearing in equations (34) are the ones obtained via FE modelling of the combined soil–structure system.

Considering a unit-amplitude harmonic acceleration input, which, for the sake of simplicity, is identical at all support points but simply time-shifted according to a given apparent propagation velocity $\vec{\mathbf{V}}_a$ in the free-field plane, we can write the free-field motion vector as

$$\mathbf{u} = -\frac{1}{\omega^2}\boldsymbol{\tau} e^{i\omega t}; \qquad \boldsymbol{\tau} = \begin{Bmatrix} e^{-i\omega\tau_1} \\ e^{-i\omega\tau_2} \\ \vdots \\ e^{-i\omega\tau_{ns}} \end{Bmatrix} \tag{35}$$

where

$$\tau_j = \frac{\vec{V}_a \cdot \vec{d}_j}{V_a^2} \tag{36}$$

while ns is the number of support points and $\vec{d}_j$ the distance of the jth support from a reference point. Upon substitution of equation (35) in (34) the preceding equations can be rewritten as

$$\mathbf{m}\ddot{\mathbf{q}}_a + \mathbf{c}\dot{\mathbf{q}}_a + \mathbf{k}\mathbf{q}_a = \left[-\begin{bmatrix} \mathbf{m}_{sc}^{(s)} \\ \mathbf{m}_{cc}^{(s)} \\ \mathbf{0} \end{bmatrix} - \frac{1}{i\omega}\begin{bmatrix} \mathbf{c}_{sc}^{(s)} \\ \mathbf{c}_{cc}^{(s)} \\ \mathbf{0} \end{bmatrix} + \frac{1}{\omega^2}\begin{bmatrix} \mathbf{k}_{sc}^{(s)} \\ \mathbf{k}_{cc}^{(s)} \\ \mathbf{0} \end{bmatrix} \right] \boldsymbol{\tau} e^{i\omega t} \tag{37}$$

In this case the frequency-response functions relating the system configuration (added motion) to the free-field acceleration at the reference point can be expressed as

$$\bar{\mathbf{q}}_a(\omega) = \mathbf{H}(\omega) \left[-\begin{bmatrix} \mathbf{m}_{sc}^{(s)} \\ \mathbf{m}_{cc}^{(s)} \\ \mathbf{0} \end{bmatrix} - \frac{1}{i\omega}\begin{bmatrix} \mathbf{c}_{sc}^{(s)} \\ \mathbf{c}_{cc}^{(s)} \\ \mathbf{0} \end{bmatrix} + \frac{1}{\omega^2}\begin{bmatrix} \mathbf{k}_{sc}^{(s)} \\ \mathbf{k}_{cc}^{(s)} \\ \mathbf{0} \end{bmatrix} \right] \boldsymbol{\tau} \tag{38}$$

Considering a structural response parameter (internal force or stress component) this can be expressed now, combining free-field and added motion, as follows:

$$s(t) = \mathbf{b}^T\mathbf{q}_a + \mathbf{d}^T\mathbf{u} \tag{39}$$

where $\mathbf{d}$ is a new suitable stiffness vector; the frequency-response function of the $s(t)$ parameter takes the form

$$\bar{s}(\omega) = \mathbf{b}^T\bar{\mathbf{q}}_a(\omega) - \frac{1}{\omega^2}\mathbf{d}^T\boldsymbol{\tau} \tag{40}$$

where $\bar{\mathbf{q}}_a(\omega)$ is expressed by equations (38).

Note that, if the CVLH model is adopted, the structural damping matrices appearing in equations (38) are as follows

$$\mathbf{c}_{\mathrm{sc}}^{(\mathrm{s})} = \mathrm{i}\,\mathrm{sign}\,(\omega)\mu^{(\mathrm{s})}\mathbf{k}_{\mathrm{sc}}^{(\mathrm{s})}; \qquad \mathbf{c}_{\mathrm{cc}}^{(\mathrm{s})} = \mathrm{i}\,\mathrm{sign}\,(\omega)\mu^{(\mathrm{s})}\mathbf{k}_{\mathrm{cc}}^{(\mathrm{s})} \tag{41}$$

Assuming now lumped-parameter soil modelling, the ground configuration disappears from the previous equations and equation (38) takes the simplified form

$$\bar{\mathbf{q}}_{\mathrm{a}}(\omega) = \begin{Bmatrix} \bar{\mathbf{q}}^{(\mathrm{s})} \\ \bar{\mathbf{q}}_{\mathrm{a}}^{(\mathrm{c})} \end{Bmatrix} = \mathbf{H}(\omega)\left[-\begin{bmatrix} \mathbf{m}_{\mathrm{sc}}^{(\mathrm{s})} \\ \mathbf{m}_{\mathrm{cc}}^{(\mathrm{s})} \end{bmatrix} - \frac{1}{\mathrm{i}\omega}\begin{bmatrix} \mathbf{c}_{\mathrm{sc}}^{(\mathrm{s})} \\ \mathbf{c}_{\mathrm{cc}}^{(\mathrm{s})} \end{bmatrix} + \frac{1}{\omega^2}\begin{bmatrix} \mathbf{k}_{\mathrm{sc}}^{(\mathrm{s})} \\ \mathbf{k}_{\mathrm{cc}}^{(\mathrm{s})} \end{bmatrix}\right]\boldsymbol{\tau} \tag{42}$$

A classical approach to the formation of a viscous damping matrix for such a system (see e.g. Reference 16) starts from the decomposition of the structural motion into pseudo-static and dynamic components

$$\mathbf{q}^{(\mathrm{s})} = \mathbf{q}_{\mathrm{p}}^{(\mathrm{s})} + \mathbf{q}_{\mathrm{d}}^{(\mathrm{s})} \tag{43}$$

where the pseudo-static motion can be obtained, neglecting dynamic effects and imposing contact points displacements as

$$\mathbf{q}_{\mathrm{p}}^{(\mathrm{s})} = -\,\mathbf{k}_{\mathrm{ss}}^{(\mathrm{s})^{-1}}\mathbf{k}_{\mathrm{sc}}^{(\mathrm{s})}\mathbf{q}^{(\mathrm{c})} = \mathbf{N}\mathbf{q}^{(\mathrm{c})} \tag{44}$$

At this point it can be assumed that structural dissipation is entirely related to dynamic motion; under this assumption the FSMD procedure (see Section 3.1) can be used by simply modifying the coordinate transformation (16), thus leading to the following steps:

(1) The damping matrix $\bar{\mathbf{c}}_{\mathrm{V}}^{(\mathrm{sf})}$ for the fixed-base structure is computed from the damping factor $\mu^{(\mathrm{s})}$, according to expression (15).
(2) The transformation

$$\dot{\mathbf{q}}_{\mathrm{d}}^{(\mathrm{s})} = \gamma\dot{\mathbf{q}} \tag{45}$$

is performed, where matrix γ can be obtained, from expressions (43) and (44) by writing

$$\dot{\mathbf{q}}_{\mathrm{d}}^{(\mathrm{s})} = \dot{\mathbf{q}}^{(\mathrm{s})} - \dot{\mathbf{q}}_{\mathrm{p}}^{(\mathrm{s})} = \dot{\mathbf{q}}^{(\mathrm{s})} - \mathbf{N}\dot{\mathbf{q}}^{(\mathrm{c})} \tag{46}$$

so that

$$\gamma = [\mathbf{I} \;\; -\mathbf{N}] \tag{47}$$

(3) To define the structure damping matrix in the $\mathbf{q}$ co-ordinate system $\mathbf{c}_{\mathrm{V}}^{(\mathrm{s})}$, the Rayleigh dissipation function is then expressed, according to the above hypothesis, as

$$D^{(\mathrm{s})} = \tfrac{1}{2}\dot{\mathbf{q}}_{\mathrm{d}}^{(\mathrm{s})\mathrm{T}}\bar{\mathbf{c}}_{\mathrm{V}}^{(\mathrm{sf})}\dot{\mathbf{q}}_{\mathrm{d}}^{(\mathrm{s})} = \tfrac{1}{2}\dot{\mathbf{q}}^{\mathrm{T}}\gamma^{\mathrm{T}}\bar{\mathbf{c}}_{\mathrm{V}}^{(\mathrm{sf})}\gamma\dot{\mathbf{q}} \tag{48}$$

which implicitly defines $\mathbf{c}_{\mathrm{V}}^{(\mathrm{s})}$ as

$$\mathbf{c}_{\mathrm{V}}^{(\mathrm{s})} = \gamma^{\mathrm{T}}\bar{\mathbf{c}}_{\mathrm{V}}^{(\mathrm{sf})}\gamma \tag{49}$$

(4) The structural damping matrix $\mathbf{c}_{\mathrm{V}}^{(\mathrm{s})}$ is added to the ground damping matrix $\mathbf{c}_{\mathrm{V}}^{(\mathrm{g})}$, which is formed according to the same criteria as mentioned for the single-mat foundation, to form the total viscous damping matrix

$$\mathbf{c}_{\mathrm{V}} = \mathbf{c}_{\mathrm{V}}^{(\mathrm{s})} + \mathbf{c}_{\mathrm{V}}^{(\mathrm{g})} \tag{50}$$

Regarding the CSMD procedure (29)–(31) one can note that it can be applied with no modification to the case of multiply-supported structures; it is also worth noting that in this case, given that equations (34) refer to absolute motion, obtaining the structural damping matrix on the basis of the combined system properties gives rise to damping terms which are proportional to absolute velocities.

As a simple example, the transverse vibrations of the structure in Figure 8 (named system B in the following), assumed under multiple-support (time-shifted) transverse ground acceleration has been studied; the properties of system B are summarized in Table III. Ground hysteretic damping is assumed to be zero.

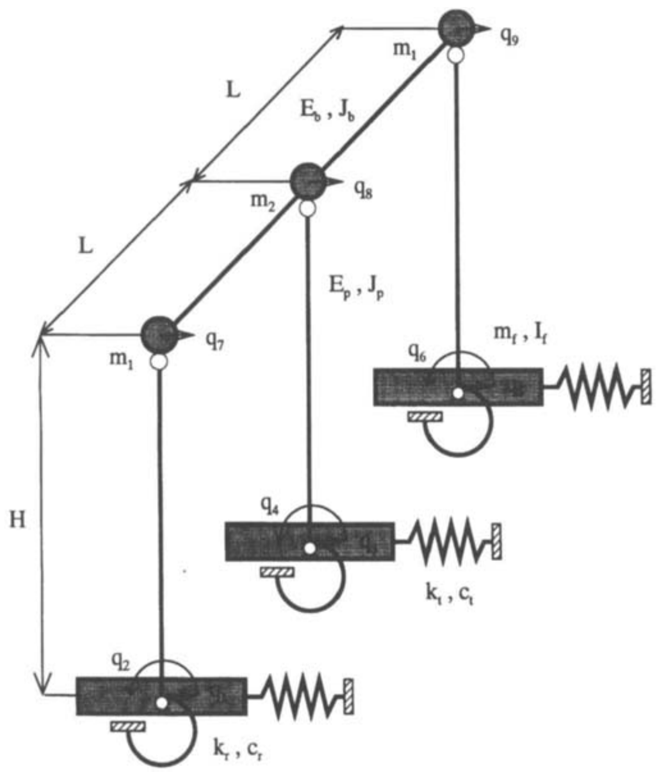

Figure 8. System B. Dynamic model

Table III. System B: mechanical properties

E_p	J_p	E_b	J_b	$\mu^{(s)}$
3×10^7 kN/m^2	8·75 m^4	4×10^7 kN/m^2	60·56 m^4	0·10
m_1	m_2	m_f	I_f	L
1155×10^3 kg	1413×10^3 kg	1214×10^3 kg	$11\,517\times10^3$ kg m^2	40 m
k_t	k_r	c_t	c_r	H
$2{\cdot}2\times10^6$ kN/m	$6{\cdot}0\times10^8$ kN m	$38\,011\times10^3$ kg/s	$2{\cdot}604\times10^9$ kgm^2/s	20 m

Frequency-response functions for response parameters of interest have been computed and compared for the CVLH, FSMD (equations (45)–(50)) and CSMD ((29)–(31)) damping models. Figures 9 and 10 show, as an example, the frequency-response curves relating the reference contact point free-field acceleration to the bending moment at the base of the centre column; curves are shown for two different values of the apparent propagation velocity, namely 1000 and 200 m/s.

It can be noted, from the quoted figures, that the CSMD procedure gives better results in the intermediate and upper frequency range, especially for the lower value of propagation velocity (Figure 10). In the low-frequency range, however, the CSMD method gives rise to a spurious increase in the response function; the increase is due, in this case, to damping forces dependent on absolute velocities. Note that the latter quantities, for constant amplitude free-field acceleration, become unbounded at low frequencies; for this

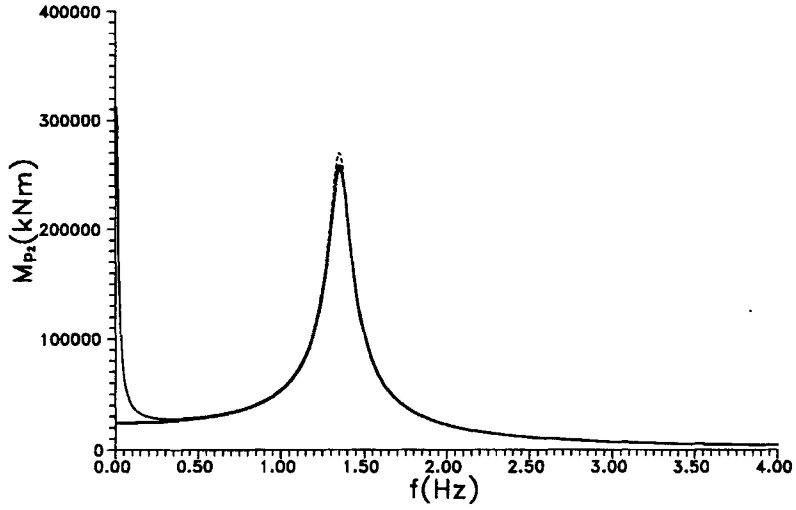

Figure 9. System B. Frequency-response function amplitude for bending moment M_{p2}. $V_a = 1{\cdot}0$ km/s: (▬) CVLH, (——) CSMD, (- - - -) FSMD

reason no advantage is gained, for the system under multiple-support input, from dropping the damping term from the r.h.s. of equations (42).

On the other hand, it can be considered that, whichever ground motion model is adopted, since free-field displacement must be bounded at low frequencies, ground velocities must tend to zero in the same range, so that the spurious low-frequency components of the CSMD response functions will have less importance on the output spectra of the response parameters of interest. This consideration has been tested by considering, for ground acceleration power spectrum, the well-accepted filtered Kanai–Tajimi model

$$S_{\ddot{u}}(\omega) = S_0 \frac{1 + 4\zeta_g^2(\omega/\omega_g)^2}{[1-(\omega/\omega_g)^2]^2 + 4\zeta_g^2(\omega/\omega_g)^2} \frac{(\omega/\omega_f)^4}{[1-(\omega/\omega_f)^2]^2 + 4\zeta_f^2(\omega/\omega_f)^2} \tag{51}$$

with $S_0 = 1$ and assuming the parameters, as suggested by Ruiz and Penzien,[17]

$$\omega_g = 15{\cdot}46 \text{ rad/s}, \qquad \zeta_g = 0{\cdot}623, \qquad \omega_f = 1{\cdot}636 \text{ rad/s}, \qquad \zeta_f = 0{\cdot}619$$

Output power spectra have been obtained according to the single-input stationary response relation

$$S_s(\omega) = |\bar{s}(\omega)|^2 S_{\ddot{u}}(\omega) \tag{52}$$

in which $\bar{s}(\omega)$ is the frequency-response function defined by equations (40) and (42). The output power spectrum is compared in Figure 11, for the case $V_a = 200$ m/s, to the one obtained by the CVLH model, showing significant discrepancies only in a narrow frequency band characterized by small spectral amplitudes.

3.3. Structures with internal damping devices

Increasing difficulties are encountered, in forming an equivalent viscous damping matrix, when the system at study encompasses internal dissipation devices of viscous type. As a simple example, one can consider the adoption of viscoelastic bearings (see Figure 12) for supporting the upper beam in system B; each of the isolators in the figure is thought as the assemblage of a linear spring of stiffness $k^{(i)}$ and a viscous dashpot of coefficient $c^{(i)}$ acting in parallel. The properties of the system in Figure 12 (named system C in the following) are summarized in Table IV; the values not indicated in the table are the same as for system B. Another typical example of arrangements of this type is encountered in the study of the behaviour of vibrating machines supported by isolated decks.

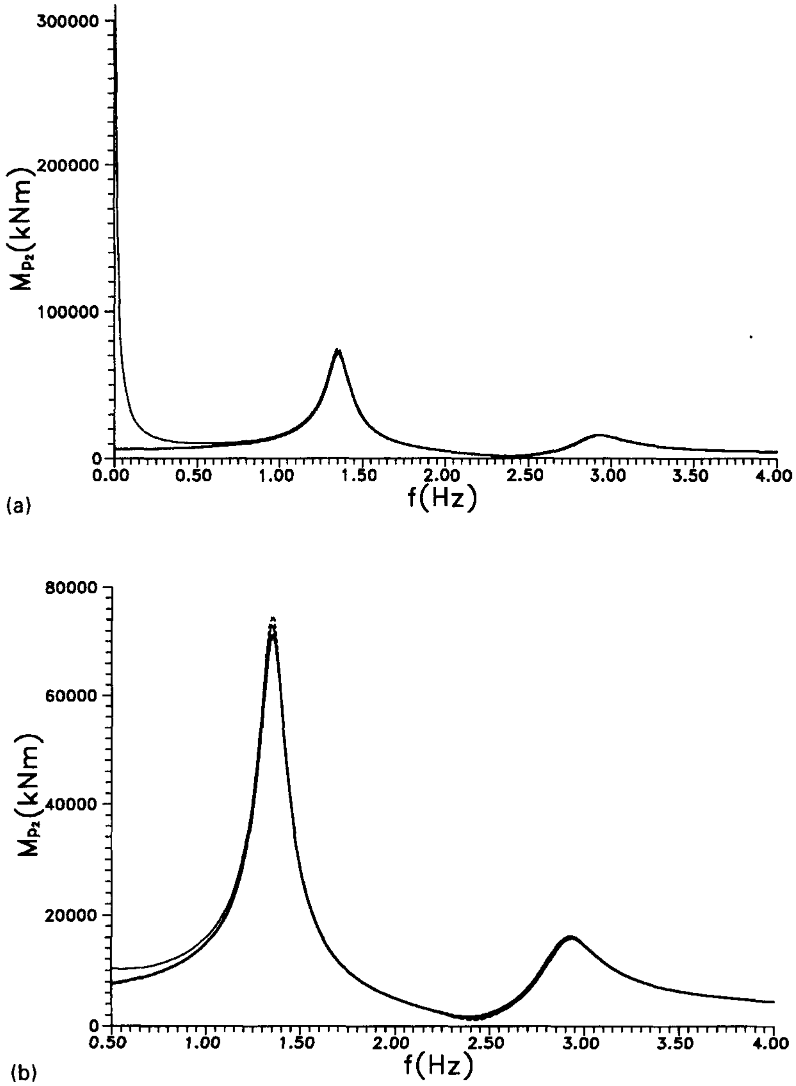

Figure 10. (a) System B. Frequency-response function amplitude for bending moment M_{p2}. $V_a = 0{\cdot}2$ km/s: (▬) CVLH, (——) CSMD, (- - - -) FSMD. (b) Enlarged portion of Figure 10(a)

As to the application of the FSMD method to this case, it can be observed that the procedure is largely based (see again Reference 15) on the existence of a well-defined primary–secondary subsystem cascade (e.g. soil–structure or structure-equipment) and on the hypothesis of homogeneous hysteretic damping for the secondary subsystem. These conditions are very difficult to meet for a system of this type, unless very arbitrary simplifying assumptions are introduced.

On the contrary, application of the CSMD technique to this case is straightforward under the, remarkably sound, assumption that dissipation due to hysteresis in the ground and in the structural system (with no dampers) is of proportional type. This leads to the following updates of expressions (29) and (31):

$$\zeta_{j,\mathrm{H}} = \frac{1}{2}\frac{\mu^{(s)}E^{(s)}_{\mathrm{MAX},j} + \mu^{(g)}E^{(g)}_{\mathrm{MAX},j} + \mu^{(i)}E^{(i)}_{\mathrm{MAX},j}}{E^{(s)}_{\mathrm{MAX},j} + E^{(g)}_{\mathrm{MAX},j} + E^{(i)}_{\mathrm{MAX},j}} \tag{53}$$

$$\mathbf{c}_{\mathrm{V}} = \mathbf{c}_{\mathrm{V,H}} + \mathbf{c}^{(g)}_{\mathrm{V}} + \mathbf{c}^{(i)}_{\mathrm{V}} \tag{54}$$

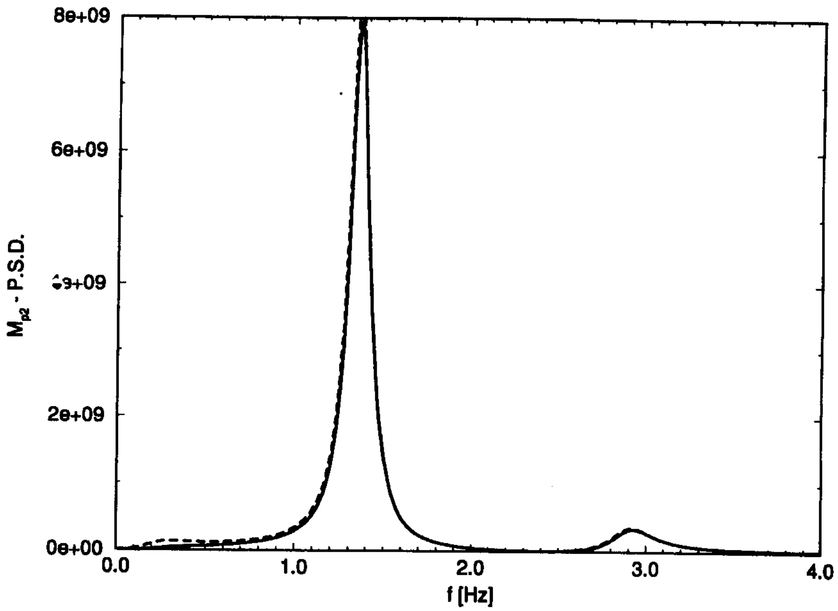

Figure 11. System B. Power spectral density for bending moment M_{p2}. $V_a = 0{\cdot}2$ km/s: (——) CVLH, (----) CSMD

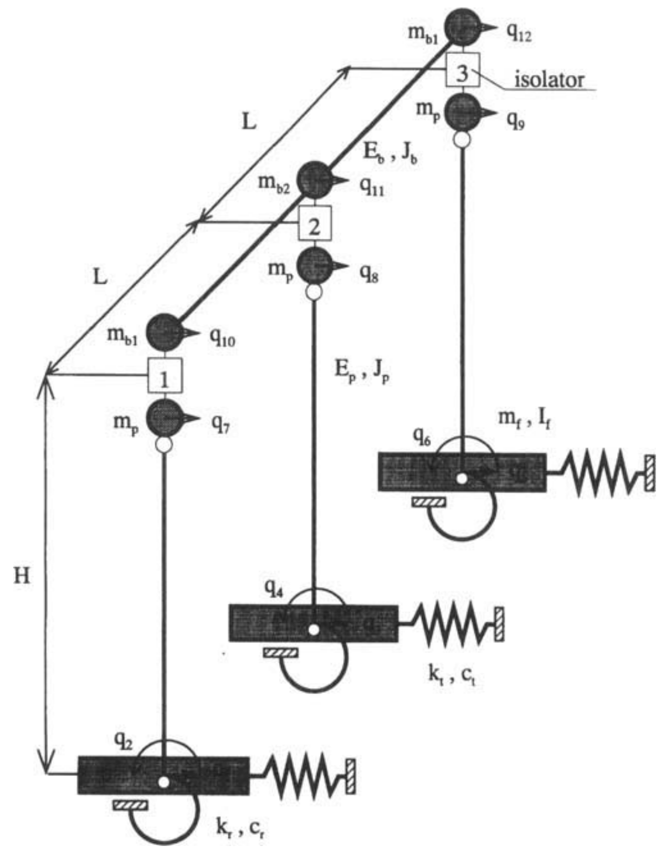

Figure 12. System C. Dynamic model

Table IV. System C: mechanical properties

m_p	m_{b1}	m_{b2}	$k^{(i)}$	$c^{(i)}$
223×10^3 kg	595×10^3 kg	1190×10^3 kg	7830 kN/m	997×10^3 kg/s

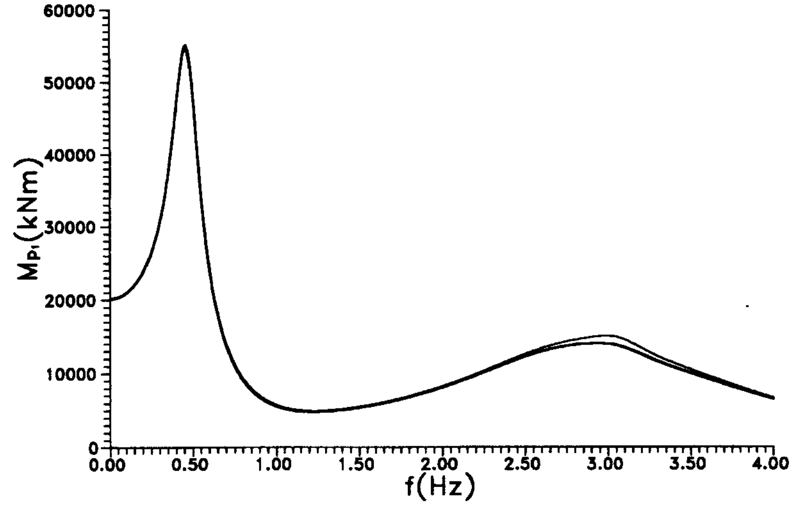

Figure 13. System C. Frequency-response function amplitude for bending moment M_{p1}. $V_a = \infty$: (▬) CVLH, (——) CSMD

where $\mathbf{c}_V^{(i)}$ and $\mu^{(i)}$ denote, respectively, the viscous matrix and the hysteretic damping factor characterizing the isolation device; note that the hysteretic term is associated to the presence of the deformable elements acting in parallel to the viscous dampers. For the system in Figure 12 elastic elements have been designed by imposing a value of 0·5 Hz to the rigid-body natural frequency of the beam, that is by computing the stiffness of each element $k^{(i)}$ from the equation

$$\frac{1}{2\pi}\sqrt{\frac{3k^{(i)}}{2m_{b1} + m_{b2}}} = 0{\cdot}5 \text{ Hz}$$

As to the value of the viscous coefficient of each isolating device, it has been subsequently stated according to the condition

$$c^{(i)} = \tfrac{1}{3}\left(2\zeta^{(i)}\sqrt{3k^{(i)}(2m_{b1} + m_{b2})}\right)$$

where $\zeta^{(i)} = 0{\cdot}2$ has been assumed. The hysteretic factor $\mu^{(i)}$ has been assumed to be zero.

Note that a criterion similar to the CSMD here described has been applied by Kawashima and Unjoh[18] for a system with internal isolating devices: in their model, however, soil–structure interaction was neglected.

Frequency-response functions have been computed, under the same criteria as adopted for the example in the preceding section, for system C. The results obtained according to the CSMD model have been compared to the ones computed by assuming the CVLH model. Adoption of the latter model results, in this case, in a frequency-response matrix of the following type:

$$\mathbf{H}(\omega) = [-\omega^2\mathbf{m} + \mathbf{k} + \mathrm{i}\,\mathrm{sign}(\omega)[\mu^{(s)}\mathbf{k}^{(s)} + \mu^{(i)}\mathbf{k}^{(i)} + \mu^{(g)}\mathbf{k}^{(g)}] + \mathrm{i}\omega[\mathbf{c}_V^{(g)} + \mathbf{c}_V^{(i)}]]^{-1} \qquad (55)$$

where $\mathbf{k}^{(i)}$ is the contribution of the isolating devices to the total stiffness matrix.

Figures 13 and 14 show the frequency-response curves relating the reference contact point free-field acceleration to bending moments at column 1; curves are shown for the case of uniform excitation and for

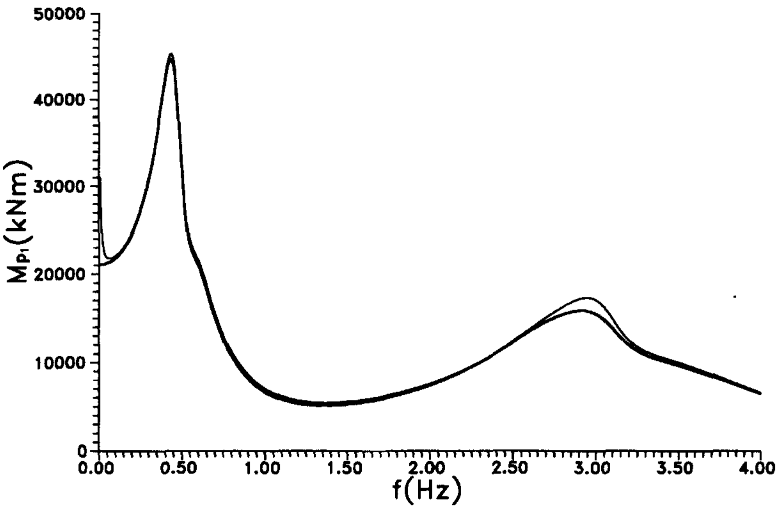

Figure 14. System C. Frequency-response function amplitude for bending moment M_{p1}. $V_a = 0{\cdot}2$ km/s: (▬) CVLH, (——) CSMD

a value of the apparent propagation velocity equal to 200 m/s. For the uniform seismic input the inertial excitation model (equation (24) with no damping term) has been used to eliminate low-frequency errors.

As it can be noted, the two models give almost identical results for the first amplitude peak, regardless of the excitation type (uniform or not). For this reason the elastic forces in the isolators (not shown here), which are almost entirely dependent on the first mode, are very closely approximated by the CSMD model. Significant discrepancies appear in the second response peak, especially for the non-uniform excitation case; however, given the difficulties associated with dissipation modelling in a system of this type, the approximation still appears acceptable. As it concerns low-frequency errors the same comments as made in the previous section hold.

4. CONCLUSIONS

The problem of forming consistently viscous damping matrices for modelling dissipation properties of linear systems has been treated; reference has been made to frequently encountered situations, such as soil–structure interacting systems or systems with internal isolation devices, where different dissipation mechanisms, namely viscous and hysteretic, are present.

Some accepted techniques for building viscous matrices which are equivalent to hysteretic structural effects have been discussed and tested; it has been shown how these techniques, which are based upon the use of normal modes of the fixed-base or unrestrained structural system, can lead to significant errors in response computations due to the shift in natural frequencies which is caused by ground deformability. For this reason a method based upon the normal modes of the combined system has been proposed and tested; particular attention has been devoted to the problems which arise, in the seismic case, due to the particular type of excitation (motion of the constraints) and to the techniques adopted for defining equivalent force vectors based upon free-field surface motion.

ACKNOWLEDGEMENT

This research has been done with the contribution of the Italian Ministry for University and Scientific and Technological Research (MURST).

REFERENCES

1. T. Igusa, A. Der Kiureghian and J. L. Sackman, 'Modal decomposition method for stationary response of non-classically damped systems', *Earthquake eng. struct. dyn.* **12**, 121–136 (1984).
2. A. S. Veletsos and C. E. Ventura, 'Modal analysis of non-classically damped linear systems', *Earthquake eng. struct. dyn.* **14**, 217–243 (1986).
3. C. E. Ventura and A. S. Veletsos, 'Steady-state and transient responses of non-classically damped linear systems', *Earthquake eng. struct. dyn.* **14**, 595–608 (1986).
4. G. Borino and G. Muscolino, 'Mode-superposition methods in dynamic analysis of classically and non-classically damped linear systems', *Earthquake eng. struct. dyn.* **14**, 705–717 (1986).
5. F. Perotti, 'Analytical and numerical techniques for the dynamic analysis of non-classically damped linear systems', *Soil dyn. earthquake eng.* **13**, 197–212 (1994).
6. J. A. Inaudi and J. M. Kelly, 'Linear hysteretic damping and the Hilbert transform', *J. eng. mech. ASCE* **121**, 626–632 (1995).
7. S. H. Crandall, 'The role of damping in vibration theory', *J. sound. vib.* **11**, 3–18 (1970).
8. R. H. Scanlan, 'Linear damping models and causality in vibrations', *J. sound. vib.* **13**, 499–503 (1970).
9. C. W. Bert, 'Material damping: an introductory review of mathematical models, measures and experimental techniques', *J. sound. vib.* **29**, 129–153 (1973).
10. A. Feriani and F. Perotti, 'Equivalent viscous damping for the dynamic analysis of M.D.O.F. systems', Universita' degli Studi di Brescia, Department of Civil Engineering, *Technical Report 1-96*, 1996.
11. C. H. Page, *Physical Mathematics*, Van Nostrand Company, New York, 1955.
12. D. C. Champeney, *A Handbook of Fourier Theorems*, Cambridge University Press, Cambridge, 1989.
13. J. M. Roesset, R. V. Whitman and R. Dobry, 'Modal analysis for structures with foundation interaction', *J. struct. div. ASCE* **99**, 399–415 (1973).
14. E. L. Wilson and J. Penzien, 'Evaluation of orthogonal damping matrices', *Int. j. numer. methods eng.* **4**, 5–10 (1972).
15. R. W. Clough and J. Penzien, *Dynamics of Structures*, McGraw-Hill Kogakusha Ltd., Tokyo 1975.
16. G. Muscolino, 'Dynamic response of multiply connected primary-secondary systems', *Earthquake eng. struct. dyn.* **19**, 205–216 (1990).
17. P. Ruiz and J. Penzien, *Probabilistic Study of the Behaviour of Structures During Earthquakes*, Earthquake Engineering Research Center, University of California, Berkeley, CA, 1969.
18. K. Kawashima and S. Unjoh, 'Seismic response control of bridges by variable dampers', *J. struct. eng. ASCE* **120**, 2583–2601 (1994).